Ukrainian Journal of Physical Optics
ISSUE 1
2026

POLARIZATION–DEPENDENT ACOUSTO-OPTIC EFFICIENCY IN OPTICALLY ACTIVE BIAXIAL α-HIO_3 CRYSTALS

O. MYS, M. KOSTYRKO AND R. VLOKH*

O.G.Vlokh Institute of Physical Optics of the Ivan Franko National University of Lviv,
23 Dragomanov Str., lviv, 79005, Ulraine
*Corresponding author: r_vlokh@ukr.net

Received: 21.01.2026

Abstract. The effect of polarization of the incident optical wave on the effective elasto-optic coefficient and the acousto-optic figure of merit in optically active, optically biaxial α-HIO_3 crystals is analyzed in the present work. It has been revealed that the increase in both parameters occurs when the polarization of the incident optical wave aligns with the polarization of the eigenwaves at the interaction with the quasi-longitudinal acoustic wave. The acousto-optic figure of merit for the case of acousto-optic interaction with quasi-longitudinal AW increases more than two times, reaching almost the same value as the maximal one in the *XZ* plane of acousto-optic interaction. It has been found that at the fifth and sixth types of acousto-optic interactions with a pure transverse acoustic wave, the acousto-optic diffraction is only possible due to the optical activity and ellipticity of the eigenwaves. In particular, for the sixth interaction type, the acousto-optic figure of merit caused solely by the eigenwaves' ellipticity reaches 13.4×10^{-15} s^3/kg.

Keywords: acousto-optic figure of merit, biaxial crystals, optical activity, α-HIO_3 crystal
UDC: 535.4, 535.012.22, 534.2
DOI: 10.3116/16091833/Ukr.J.Phys.Opt.2026.01110

1. Introduction

Acousto-optic (AO) Bragg diffraction is the effect of optical wave diffraction on a phase grating of refractive index created by the acoustic wave (AW) through the elasto-optic (EO) effect [1-5]. The many applications of AO diffraction make this effect quite important in optoelectronics. AO diffraction can be used for deflecting optical radiation in scanners by changing the AW frequency, modulating the intensity of the diffracted wave by adjusting the amplitude of the AW, and in AO tunable filters, among other uses.

One of the most important characteristics of AO Bragg diffraction is the AO figure of merit, defining the efficiency of diffraction, i.e., the portion of optical intensity deflected into the diffraction maximum. The diffraction efficiency of AO Bragg diffraction is determined by the relation:

$$\eta = I / I_0 = \sin^2\left(\frac{\pi}{\lambda\cos\theta_B}\sqrt{M_2 P_a \frac{l}{2b}}\right), \quad (1)$$

where I and I_0 are the intensities of respectively diffracted and incident light, λ the wavelength of optical radiation, θ_B the Bragg angle, P_a the AW power, M_2 the AO figure of merit, l the interaction length, and b the height of the acoustic beam. In its turn, the M_2 factor is determined as

$$M_2 = \frac{n_i^3 n_d^3 p_{eff}^2}{\rho v_{kl}^3}, \quad (2)$$

where n_i and n_d denote the refractive indices of respectively incident and diffracted waves,

p_{eff} the effective EO coefficient, ρ the material density, and v_{kl} the AW velocity (the indices k and l correspond to the directions of propagation and polarization of the AW). Therefore, increasing the AO figure of merit, which naturally reduces the power of AW and energy consumption, can be achieved by enhancing the effective EO coefficient. Although lowering the AW speed can also produce the same effect, it decreases the repetition rate and reduces the response speed of AO devices.

The increase in the effective EO coefficient can be achieved by searching for optimal directions and polarizations of interacting optical and acoustic waves within the optical and acoustic anisotropy (see, e.g.,[6,7]). However, in our recent works [8,9], we have shown that optical activity in these materials can significantly enhance their AO figure of merit. This occurs because the ellipticity of interacting optical eigenwaves approaches unity near the optic axis, causing additional EO tensor components to contribute to the effective EO coefficient. This enhancement has been demonstrated in cubic optically active crystals and optically uniaxial crystals [9]. It has been shown that in cubic system crystals, considering the circular polarization of the incident optical wave results in an inflation in the characteristic surface of the AO figure of merit. Conversely, in optically uniaxial crystals, this consideration leads to a peak-like increase of the AO figure of merit when the incident wave propagates along the optical axis, where the eigenwaves become purely circularly polarized [1]. The enhancement of AO efficiency when the polarization ellipticity of the incident optical wave matches that of one of the eigenwaves has been experimentally demonstrated for patratellurite crystals [10]. Meanwhile, optically biaxial crystals may exhibit greater variations of this effect due to symmetry lowering and the presence of additional independent components of the elastic and EO tensors [11]. It is clear that if the optical activity is non-zero along both optical axes, the enhancement of the AO figure of merit will manifest along both directions, thereby expanding the possible propagation directions for the incident optical wave. Therefore, this work focuses on studying how the ellipticity of optical eigenwaves influences the effective EO coefficient and AO figure of merit in optically biaxial crystals, using α-HIO_3 crystals as an example.

2. Method of analysis

In this work, we analyze the anisotropy of effective EO coefficients and AO figure of merit for isotropic AO interaction. The analysis follows the same scheme as in our previous works (see e.g., [6,8]). Specifically, we examine six isotropic types of AO interactions: I - interaction of the optical wave with a larger refractive index with quasi-longitudinal (QL) AW; II - interaction of the optical wave with a smaller refractive index with QL AW; III - interaction of the optical wave with a larger refractive index with quasi-transverse (QT_1) AW, polarized in the plane of AO interaction; IV - interaction of the optical wave with a smaller refractive index with QT_1 AW; V - interaction of the optical wave with a larger refractive index with pure-transverse (PT_2) AW, polarized perpendicular to the plane of AO interaction; and VI - interaction of the optical wave with a smaller refractive index with PT_2 AW. The analysis was conducted in the crystallographic plane that coincides with the optical-axes plane of α-HIO_3 crystals.

The α-HIO_3, the stable polymorph of iodic acid, crystallizes in the orthorhombic system with the non-centrosymmetric space group $P2_12_12_1$ [12]. The lattice constants are determined as a=5.5379 A, b=5.8878 A, and c= 7.7333 A [12]. There are four molecules in a unit cell, and the density is 4630 kg/m³. The crystals are negative biaxial ($n_Z \approx n_Y > n_X$) with

$Z = b$, $Y = -c$, $X = a$. However, in many works, another correspondence between the crystallographic (a, b, c) and crystal physics (X, Y, Z) coordinate systems is used (see e.g. [13]): a corresponds to n_X, b to n_Y, and c to n_Z. In this case, according to [14] and using Zelmeyer's equation [14], the refractive indices are equal to $n_Z = 1.8378$, $n_Y = 1.9604$, and $n_X = 1.9865$ at λ=632.8 nm. In the negative uniaxial limit $n_X = n_Y = n_o > n_Z = n_e$: o = ordinary, e = extraordinary. In our case n_X=n_1=n_p, n_Y=n_2=n_m and n_Z=n_3=n_g. The acute bisectrix is the Z axis (i.e., [001] direction) and the optic axial angle in the XZ plane is equal to $2V = 47°$ at λ=632 nm. The crystals exhibit noticeable optical activity and pronounced anisotropy. For example, at a wavelength of 632.8 nm, the components of the gyration tensor were reported to be equal: $g_{11} \approx -1.0\times10^{-4}$, $g_{22} \approx 2.6\times10^{-4}$, and $g_{33} \approx 3.3\times10^{-4}$ [15]. The components of EO tensor are equal to: p_{11}=0.406, p_{22}=0.343, p_{33}=0.334, p_{12}=0.277, p_{13}=0.304, p_{21}=0.279, p_{23}=0.305, p_{31}=0.503, p_{32}=0.310, p_{44}=0.27, p_{55}=0.2, p_{66}=0.09 [16]. The elastic stiffness tensor components, taken from [13], are as follows: C_{11}=57.0, C_{12}=6.0, C_{13}=14.6, C_{21}=6.0, C_{22}=42.9, C_{23}=11.5, C_{31}=14.6, C_{32}=11.5, C_{33}=30.0, C_{44}= 20.8, C_{55}= 16.2 and C_{66}= 17.8 GPa.

The Fresnel equation for optically biaxial crystals can be written as [11]:

$$\begin{aligned}&(X^2+Y^2+Z^2)(n_p^2X^2+n_m^2Y^2+n_g^2Z^2)\\&-n_p^2(n_m^2+n_g^2)X^2-n_m^2(n_g^2+n_p^2)Y^2-n_g^2(n_p^2+n_m^2)Z^2\,.\\&+n_p^2n_m^2n_g^2=0\end{aligned} \tag{3}$$

Solutions of this equation are the surfaces of smaller (n_s) and larger (n_l) refractive indices:

$$n_l=\sqrt{\frac{C+\sqrt{C^2-4AD}}{2A}}\,, \tag{4}$$

$$n_s=\sqrt{\frac{C-\sqrt{C^2-4AD}}{2A}}\,, \tag{5}$$

where

$$\begin{aligned}&A=n_p^2\sin^2(\theta_{ac}-\theta_B)+N_z^2\cos^2(\theta_{ac}-\theta_B)\\&C=n_p^2(n_m^2+n_g^2)\sin^2(\theta_{ac}-\theta_B)+n_g^2(n_m^2+n_p^2)\cos^2(\theta_{ac}-\theta_B)\,,\\&D=n_p^2n_m^2n_g^2\end{aligned} \tag{6}$$

and $\theta_B=0.1$ deg is the Bragg angle, θ_{ac} - is the angle between the wavevector of the AW and the X-axis (see Fig. 1). Notice that Eqs. (4,5) determine the refractive indices without accounting for the optical activity. At the accounting of the optical activity, the refractive indices are equal to [17]:

$$n_l^{oa}=n_l+\frac{G}{2\bar{n}} \text{ and } n_s^{oa}=n_s-\frac{G}{2\bar{n}}\,, \tag{7}$$

where $\bar{n}$ is the mean value of refractive indices in the direction of light propagation, and the scalar gyration parameter is equal to:

$$G=g_{11}\sin^2(\theta_a-\theta_B)+g_{33}\cos^2(\theta_a-\theta_B)\,. \tag{8}$$

The ellipticities of the eigenwaves and the effective EO coefficients can be obtained similarly to the derivation in Ref. [6]. The ellipticity of the optical eigenwaves is defined as:

$$\chi=\frac{1}{2G}\left(n_l^2-n_s^{*2}-\sqrt{(n_l^2-n_s^{*2})^2+4G^2}\right)\approx\frac{G}{n_l^2-n_s^{*2}}, \tag{9}$$

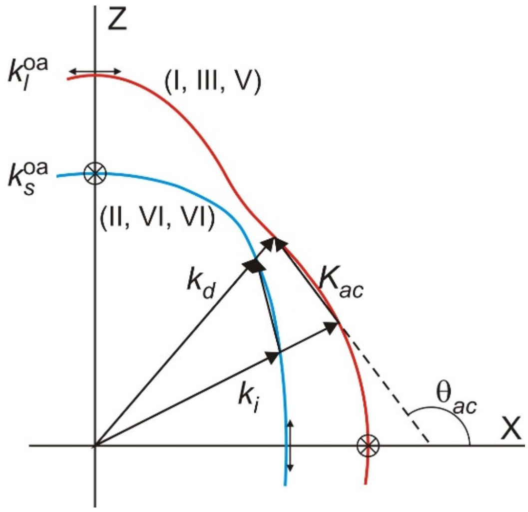

Fig. 1. Geometry of isotropic AO interaction for the α-HIO_3 crystal. $k_s^{oa}=2\pi n_s^{oa}/\lambda$, $k_l^{oa}=2\pi n_l^{oa}/\lambda$, and K_{ac} are the wavevectors of optical waves with larger and smaller refractive indices, and AW, respectively; k_i and k_d are the wavevectors of the incident and diffracted optical waves, respectively The Roman numerals indicate the types of AO interaction and their correlation to the wavevector surfaces.

The cross-section of wavevector surfaces of optically biaxial crystals by the plane of the optical axes (i.e., the *XZ* plane) is not a second-order surface (Fig. 1). Of course, in the simplest case, one can consider the intersection of two surfaces depicted as an ellipse and a circle, with the intersection points representing the outlets of the optical axes. However, these outlets are not crossing points of two second-order surfaces, but rather contact points between two higher-order surfaces. When the optical wavevector crosses the optical axis, the polarization of the eigenwave switches by 90 deg. Therefore, for a specific type of AO interaction, different (orthogonal) polarizations of incident eigenwaves must be considered at incidence angles below and above the optical axes.

The relations for effective EO coefficients in the *XZ* plane are as follows. For AO interaction with QL AW of the type I, at $336.5\,\text{deg}<\theta_{ac}<23.5\,\text{deg}$ and $156.5\,\text{deg}<\theta_{ac}<203.5\,\text{deg}$, the effective EO coefficient is determined by the equation:

$$\begin{aligned}p_{eff}^{2(I)}&=0.5\left(p_{21}\cos(\theta_{ac})\cos(\xi)+p_{23}\sin(\theta_{ac})\sin(\xi)\right)^2+\\&+0.5\chi^2\left\{\begin{array}{l}\cos^2(\theta_{ac}-\theta_B)\left\{\begin{array}{l}\left(p_{11}\cos(\theta_{ac})\cos(\xi)+p_{13}\sin(\theta_{ac})\sin(\xi)\right)^2\\+p_{55}^2\sin^2(\xi+\theta_{ac})\end{array}\right\}\\ \sin^2(\theta_{ac}-\theta_B)\left\{\begin{array}{l}\left(p_{31}\cos(\theta_{ac})\cos(\xi)+p_{33}\sin(\theta_{ac})\sin(\xi)\right)^2\\+p_{55}^2\sin^2(\xi+\theta_{ac})\end{array}\right\}\\ -\sin(2(\theta_{ac}-\theta_B))p_{55}\sin(\xi+\theta_{ac})\left\{\begin{array}{l}\left(p_{11}+p_{31}\right)\cos(\theta_{ac})\cos(\xi)\\+\left(p_{13}+p_{33}\right)\sin(\theta_{ac})\sin(\xi)\end{array}\right\}\end{array}\right\},\end{aligned} \tag{10}$$

and at $23.5\,\text{deg}<\theta_{ac}<156.5\,\text{deg}$ and $203.5\,\text{deg}<\theta_{ac}<336.5\,\text{deg}$:

$$p_{eff}^{2(I)} = 0.5\chi^2\left(p_{21}\cos(\theta_{ac})\cos(\xi)+p_{23}\sin(\theta_{ac})\sin(\xi)\right)^2 + \\ +0.5\cos^2(\theta_{ac}-\theta_B)\begin{Bmatrix}\left(p_{11}\cos(\theta_{ac})\cos(\xi)+p_{13}\sin(\theta_{ac})\sin(\xi)\right)^2 \\ +p_{55}^2\sin^2(\xi+\theta_{ac})\end{Bmatrix} \\ +0.5\sin^2(\theta_{ac}-\theta_B)\begin{Bmatrix}\left(p_{31}\cos(\theta_{ac})\cos(\xi)+p_{33}\sin(\theta_{ac})\sin(\xi)\right)^2 \\ +p_{55}^2\sin^2(\xi+\theta_{ac})\end{Bmatrix} \\ -0.5\sin(2(\theta_{ac}-\theta_B))p_{55}\sin(\xi+\theta_{ac})\begin{Bmatrix}(p_{11}+p_{31})\cos(\theta_{ac})\cos(\xi)+ \\ (p_{13}+p_{33})\sin(\theta_{ac})\sin(\xi)\end{Bmatrix}. \quad (11)$$

The effective EO coefficient for type II of AO interaction with QL AW at $336.5\,\text{deg} < \theta_{ac} < 23.5\,\text{deg}$ and $156.5\,\text{deg} < \theta_{ac} < 203.5\,\text{deg}$ is written as:

$$p_{eff}^{2(II)} = 0.5\chi^2\left(p_{21}\cos(\theta_{ac})\cos(\xi)+p_{23}\sin(\theta_{ac})\sin(\xi)\right)^2 + \\ +0.5\cos^2(\theta_{ac}-\theta_B)\left\{\left(p_{11}\cos(\theta_{ac})\cos(\xi)+p_{13}\sin(\theta_{ac})\sin(\xi)\right)^2+p_{55}^2\sin^2(\xi+\theta_{ac})\right\} \\ +0.5\sin^2(\theta_{ac}-\theta_B)\left\{\left(p_{31}\cos(\theta_{ac})\cos(\xi)+p_{33}\sin(\theta_{ac})\sin(\xi)\right)^2+p_{55}^2\sin^2(\xi+\theta_{ac})\right\} \\ -0.5\sin(2(\theta_{ac}-\theta_B))p_{55}\sin(\xi+\theta_{ac})\begin{Bmatrix}(p_{11}+p_{31})\cos(\theta_{ac})\cos(\xi) \\ +(p_{13}+p_{33})\sin(\theta_{ac})\sin(\xi)\end{Bmatrix}, \quad (12)$$

and at $23.5\,\text{deg} < \theta_{ac} < 156.5\,\text{deg}$ and $203.5\,\text{deg} < \theta_{ac} < 336.5\,\text{deg}$:

$$p_{eff}^{2(II)} = 0.5\left(p_{21}\cos(\theta_{ac})\cos(\xi)+p_{23}\sin(\theta_{ac})\sin(\xi)\right)^2 + \\ +0.5\chi^2\begin{Bmatrix}\cos^2(\theta_{ac}-\theta_B)\begin{Bmatrix}\left(p_{11}\cos(\theta_{ac})\cos(\xi)+p_{13}\sin(\theta_{ac})\sin(\xi)\right)^2 \\ +p_{55}^2\sin^2(\xi+\theta_{ac})\end{Bmatrix} \\ \sin^2(\theta_{ac}-\theta_B)\begin{Bmatrix}\left(p_{31}\cos(\theta_{ac})\cos(\xi)+p_{33}\sin(\theta_{ac})\sin(\xi)\right)^2 \\ +p_{55}^2\sin^2(\xi+\theta_{ac})\end{Bmatrix} \\ -\sin(2(\theta_{ac}-\theta_B))\mathrm{p}_{55}\sin(\xi+\theta_{ac})\begin{Bmatrix}(p_{11}+p_{31})\cos(\theta_{ac})\cos(\xi) \\ +(p_{13}+p_{33})\sin(\theta_{ac})\sin(\xi)\end{Bmatrix}\end{Bmatrix}. \quad (13)$$

For the case of the AO interaction with the QT_1 AW, the relations for effective EO coefficients in the *XZ* plane for the type III at $336.5\,\text{deg} < \theta_{ac} < 23.5\,\text{deg}$ and $156.5\,\text{deg} < \theta_{ac} < 203.5\,\text{deg}$ are as follows:

$$p_{eff}^{2(III)} = 0.5\left(p_{23}\sin(\theta_{ac})\cos(\xi)-p_{21}\cos(\theta_{ac})\sin(\xi)\right)^2 + \\ 0.5\chi^2\begin{Bmatrix}+\cos^2(\theta_{ac}-\theta_B)\begin{Bmatrix}\left(p_{13}\sin(\theta_{ac})\cos(\xi)-p_{1}\cos(\theta_{ac})\sin(\xi)\right)^2 \\ +p_{55}^2\cos^2(\xi+\theta_{ac})\end{Bmatrix} \\ +\sin^2(\theta_{ac}-\theta_B)\begin{Bmatrix}\left(p_{33}\sin(\theta_{ac})\cos(\xi)-p_{31}\cos(\theta_{ac})\sin(\xi)\right)^2 \\ +p_{55}^2\cos^2(\xi+\theta_{ac})\end{Bmatrix} \\ -\sin(2(\theta_{ac}-\theta_B))p_{55}\cos(\xi+\theta_{ac})\begin{Bmatrix}(p_{11}-p_{31})\cos(\theta_{ac})\sin(\xi) \\ +(p_{13}+p_{33})\sin(\theta_{ac})\cos(\xi)\end{Bmatrix}\end{Bmatrix}, \quad (14)$$

and at $23.5\,\text{deg} < \theta_{ac} < 156.5\,\text{deg}$ and $203.5\,\text{deg} < \theta_{ac} < 336.5\,\text{deg}$:

$$p_{eff}^{2(III)} = 0.5\chi^2\left(p_{23}\sin(\theta_{ac})\cos(\xi) - p_{21}\cos(\theta_{ac})\sin(\xi)\right)^2 + \\ +0.5\cos^2(\theta_{ac}-\theta_B)\begin{Bmatrix}\left(p_{13}\sin(\theta_{ac})\cos(\xi) - p_{11}\cos(\theta_{ac})\sin(\xi)\right)^2 \\ +p_{55}^2\cos^2(\xi+\theta_{ac})\end{Bmatrix} \\ +0.5\sin^2(\theta_{ac}-\theta_B)\begin{Bmatrix}\left(p_{33}\sin(\theta_{ac})\cos(\xi) - p_{31}\cos(\theta_{ac})\sin(\xi)\right)^2 \\ +p_{55}^2\cos^2(\xi+\theta_{ac})\end{Bmatrix} \\ -0.5\sin(2(\theta_{ac}-\theta_B))p_{55}\cos(\xi+\theta_{ac})\begin{Bmatrix}\left(p_{31}-p_{11}\right)\cos(\theta_{ac})\sin(\xi) \\ +\left(p_{13}+p_{33}\right)\sin(\theta_{ac})\cos(\xi)\end{Bmatrix} . \quad (15)$$

The effective EO coefficient for type IV of AO interaction with QT_1 AW is at $336.5\,\text{deg} < \theta_{ac} < 23.5\,\text{deg}$ and $156.5\,\text{deg} < \theta_{ac} < 203.5\,\text{deg}$ is determined as:

$$p_{eff}^{2(IV)} = 0.5\chi^2\left(p_{23}\sin(\theta_{ac})\cos(\xi) - p_{21}\cos(\theta_{ac})\sin(\xi)\right)^2 + \\ +0.5\cos^2(\theta_{ac}-\theta_B)\begin{Bmatrix}\left(p_{13}\sin(\theta_{ac})\cos(\xi) - p_{11}\cos(\theta_{ac})\sin(\xi)\right)^2 \\ +p_{55}^2\cos^2(\xi+\theta_{ac})\end{Bmatrix} \\ +0.5\sin^2(\theta_{ac}-\theta_B)\begin{Bmatrix}\left(p_{33}\sin(\theta_{ac})\cos(\xi) - p_{31}\cos(\theta_{ac})\sin(\xi)\right)^2 \\ +p_{55}^2\cos^2(\xi+\theta_{ac})\end{Bmatrix} \\ -0.5\sin(2(\theta_{ac}-\theta_B))p_{55}\cos(\xi+\theta_{ac})\begin{Bmatrix}\left(p_{31}-p_{11}\right)\cos(\theta_{ac})\sin(\xi) + \\ \left(p_{13}+p_{33}\right)\sin(\theta_{ac})\cos(\xi)\end{Bmatrix} , \quad (16)$$

and at $23.5\,\text{deg} < \theta_{ac} < 156.5\,\text{deg}$ and $203.5\,\text{deg} < \theta_{ac} < 336.5\,\text{deg}$:

$$p_{eff}^{2(IV)} = 0.5\left(p_{23}\sin(\theta_{ac})\cos(\xi) - p_{21}\cos(\theta_{ac})\sin(\xi)\right)^2 + \\ 0.5\chi^2\begin{Bmatrix} +\cos^2(\theta_{ac}-\theta_B)\begin{Bmatrix}\left(p_{13}\sin(\theta_{ac})\cos(\xi) - p_{11}\cos(\theta_{ac})\sin(\xi)\right)^2 \\ +p_{55}^2\cos^2(\xi+\theta_{ac})\end{Bmatrix} \\ +\sin^2(\theta_{ac}-\theta_B)\begin{Bmatrix}\left(p_{33}\sin(\theta_{ac})\cos(\xi) - p_{31}\cos(\theta_{ac})\sin(\xi)\right)^2 \\ +p_{55}^2\cos^2(\xi+\theta_{ac})\end{Bmatrix} \\ -\sin(2(\theta_{ac}-\theta_B))p_{55}\cos(\xi+\theta_{ac})\begin{Bmatrix}\left(p_{31}-p_{11}\right)\cos(\theta_{ac})\sin(\xi) \\ +\left(p_{13}+p_{33}\right)\sin(\theta_{ac})\cos(\xi)\end{Bmatrix}\end{Bmatrix} . \quad (17)$$

The relations for the effective EO coefficient for type V of AO interaction with PT_2 AW at $336.5\,\text{deg} < \theta_{ac} < 23.5\,\text{deg}$ and $156.5\,\text{deg} < \theta_{ac} < 203.5\,\text{deg}$ are written as:

$$p_{eff}^{2(V)} = 0.5\chi^2\begin{Bmatrix}\sin^2(\theta_{ac}-\theta_B)p_{44}^2\sin^2(\theta_{ac}) \\ +\cos^2(\theta_{ac}-\theta_B)p_{66}^2\cos^2(\theta_{ac}) \\ -0.25\sin 2(\theta_{ac}-\theta_B)\sin 2(\theta_{ac})p_{66}p_{44}\end{Bmatrix} , \quad (18)$$

and at $23.5\,\text{deg} < \theta_{ac} < 156.5\,\text{deg}$ and $203.5\,\text{deg} < \theta_{ac} < 336.5\,\text{deg}$:

$$p_{eff}^{2(V)} = 0.5\chi^2\left\{p_{66}^2\cos^2(\theta_{ac}) + p_{44}^2\sin^2(\theta_{ac})\right\} , \quad (19)$$

The relations for effective EO coefficients for type VI of AO interaction with PT_2 AW at $336.5\,\text{deg} < \theta_{ac} < 23.5\,\text{deg}$ and $156.5\,\text{deg} < \theta_{ac} < 203.5\,\text{deg}$ are as follows:

$$p_{eff}^{2(VI)} = 0.5\chi^2 \left\{ p_{66}^2 \cos^2(\theta_{ac}) + p_{44}^2 \sin^2(\theta_{ac}) \right\}, \quad (20)$$

and at $23.5\,\mathrm{deg} < \theta_{ac} < 156.5\,\mathrm{deg}$ and $203.5\,\mathrm{deg} < \theta_{ac} < 336.5\,\mathrm{deg}$:

$$p_{eff}^{2(VI)} = 0.5\chi^2 \begin{Bmatrix} \sin^2(\theta_{ac} - \theta_B) p_{44}^2 \sin^2(\theta_{ac}) + \cos^2(\theta_{ac} - \theta_B) p_{66}^2 \cos^2(\theta_{ac}) \\ -0.25 \sin 2(\theta_{ac} - \theta_B) \sin 2(\theta_{ac}) p_{66} p_{44} \end{Bmatrix}. \quad (21)$$

In these formulas, the angle between *X* axis and the displacement vector is determined as:

$$\xi(\theta_{ac}) = 0.5\,\mathrm{atan}\left(\frac{\sin 2\theta_{ac}(C_{13} + C_{55})}{\cos^2\theta_{ac}(C_{11} - C_{55}) + \sin^2\theta_{ac}(C_{55} - C_{33})} \right). \quad (22)$$

The dependence of the QL AW velocity on angle θ_{ac} can be written as:

$$\upsilon_{11} = \sqrt{\frac{C_{11}\cos^2\theta_{ac} + C_{33}\sin^2\theta_{ac} + C_{55}}{2\rho} + \frac{\sqrt{\left\{(C_{11} - C_{55})\cos^2\theta_{ac} + (C_{55} - C_{33})\sin^2\theta_{ac}\right\}^2 + (C_{13} + C_{55})\sin^2 2\theta_{ac}}}{2\rho}}. \quad (23)$$

The analogical relations for QT_1 and PT_2 AW are as follows:

$$\upsilon_{13} = \sqrt{\frac{C_{11}\cos^2\theta_{ac} + C_{33}\sin^2\theta_{ac} + C_{55}}{2\rho} - \frac{\sqrt{\left\{(C_{11} - C_{55})\cos^2\theta_{ac} + (C_{55} - C_{33})\sin^2\theta_{ac}\right\}^2 + (C_{13} + C_{55})\sin^2 2\theta_{ac}}}{2\rho}}, \quad (24)$$

and

$$\upsilon_{12} = \sqrt{\frac{C_{66}\cos^2\theta_{ac} + C_{44}\sin^2\theta_{ac}}{\rho}}, \quad (25)$$

respectively.

3. Results and discussion

The dependencies of the effective EO coefficients and AO figure of merit on the propagation direction of the QL AW for the first type of AO interaction are shown in Fig. 2a,b. It is clear that, in both cases, considering the ellipticity of the eigen optical waves caused by optical activity results in higher EO coefficients and a greater AO figure of merit when the incident optical wave propagates near the optical axes. The AO figure of merit increases from $10.8\times10^{-15}\,s^3/kg$, the value typical for a linearly polarized wave, to $23.7\times10^{-15}\,s^3/kg$, characteristic of a circularly polarized wave, due to the incident wave's polarization as the eigenwave. Nevertheless, the highest AO figure of merit achieved is slightly higher, at $28.1\times10^{-15}\,s^3/kg$, which occurs at θ_{ac}=90 and 270 deg.

For the second type of AO interaction, the dependencies of the effective EO coefficient and AO figure of merit are shown in Fig. 2 c,d. As seen, considering the circular polarization of the incident optical wave that matches the polarization of the eigenwave – under the condition of propagation along the optical axes – results in an increase in the AO figure of merit from $11.9\times10^{-15}\,s^3/kg$ to $23.8\times10^{-15}\,s^3/kg$. However, accounting for optical activity does not exceed the maximum value of the AO figure of merit without considering optical activity ($34.3\times10^{-15}\,s^3/kg$), which occurs at θ_{ac}=90 and 270 deg.

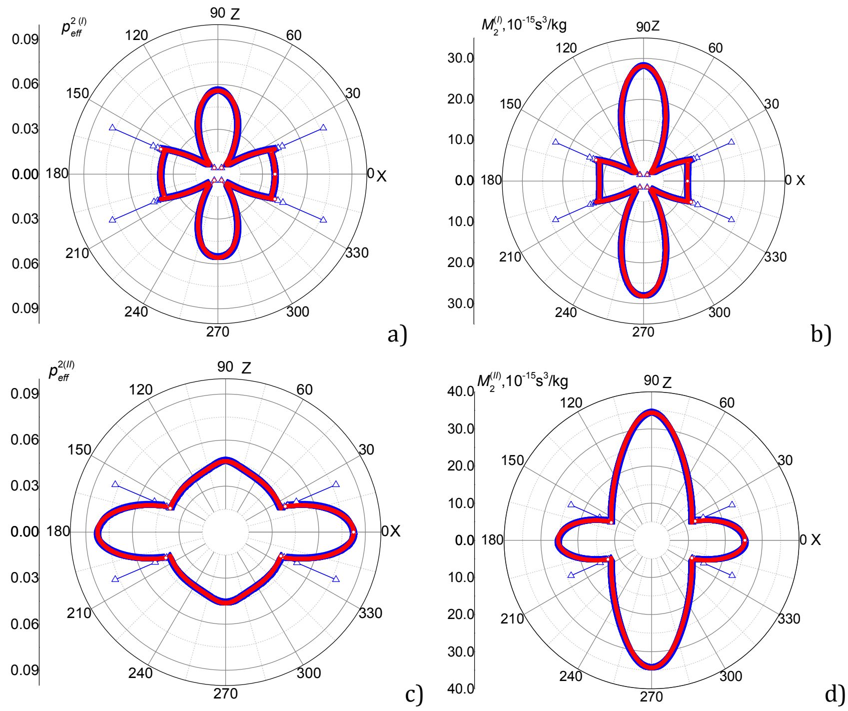

Fig. 2. Dependencies of effective EO coefficients (a, c) and AO figures of merit (b, d) on the angle θ_{ac} for the first (a, b) and second (c, d) types of AO interaction. Red circles represent the condition of neglecting the ellipticity of the eigenwaves, while blue triangles indicate the condition of considering optical activity and the ellipticity of the eigenwaves.

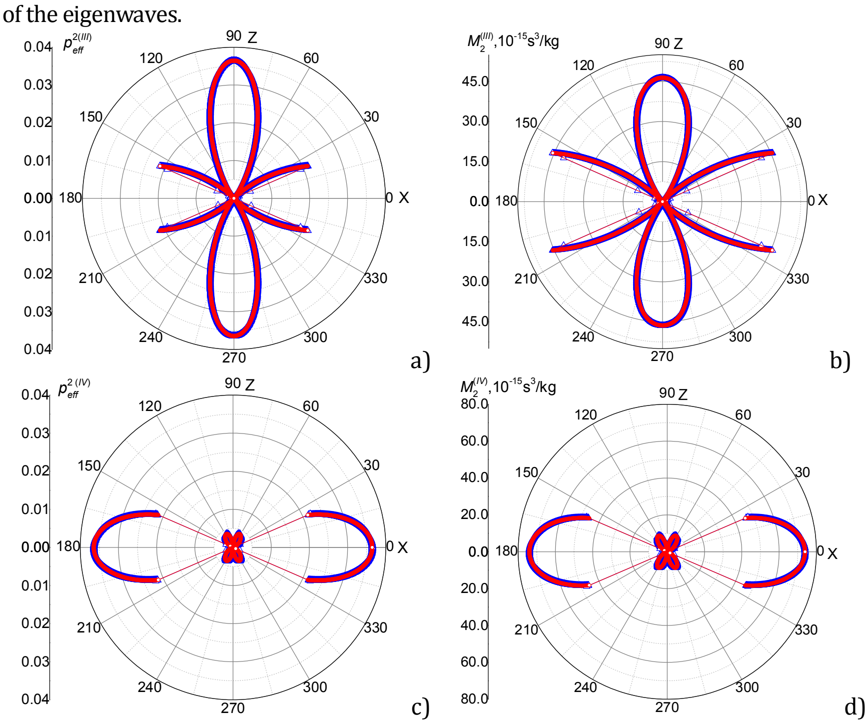

Fig. 3. Dependencies of effective EO coefficients (a, c) and AO figures of merit (b, d) on the angle θ_{ac} for the third (a, b) and fourth (c, d) types of AO interaction. Red circles represent the condition of neglecting the ellipticity of the eigenwaves, while blue triangles indicate the condition of considering optical activity and the ellipticity of the eigenwaves.

At the third and fourth types of AO interaction, the accounting of optical activity does not affect the values of the effective EO coefficient and the AO figure of merit. This may be due to the minimal influence of the term related to ellipticity in Eqs. (14-17) on the effective EO coefficient. Nonetheless, in the directions of propagation of the incident optical wave where the ellipticity of the eigenwaves is negligibly small, the AO figure of merit reaches quite high values. For example, at the third type of AO interaction at θ_{ac}= 90 and 270 deg, and when the linearly polarized incident optical wave propagates along the optical axes, the AO figure of merit is 46.3×10^{-15} s^3/kg and 45.6×10^{-15} s^3/kg, respectively. For the fourth type of interaction, the maximum value of the AO figure of merit is 74.0×10^{-15} s^3/kg at θ_{ac}= 90 and 180 deg, while at the propagation of the incident optical wave along the optical axis with and without accounting for the optical activity, the AO figure of merit is equal 46.4×10^{-15} s^3/kg.

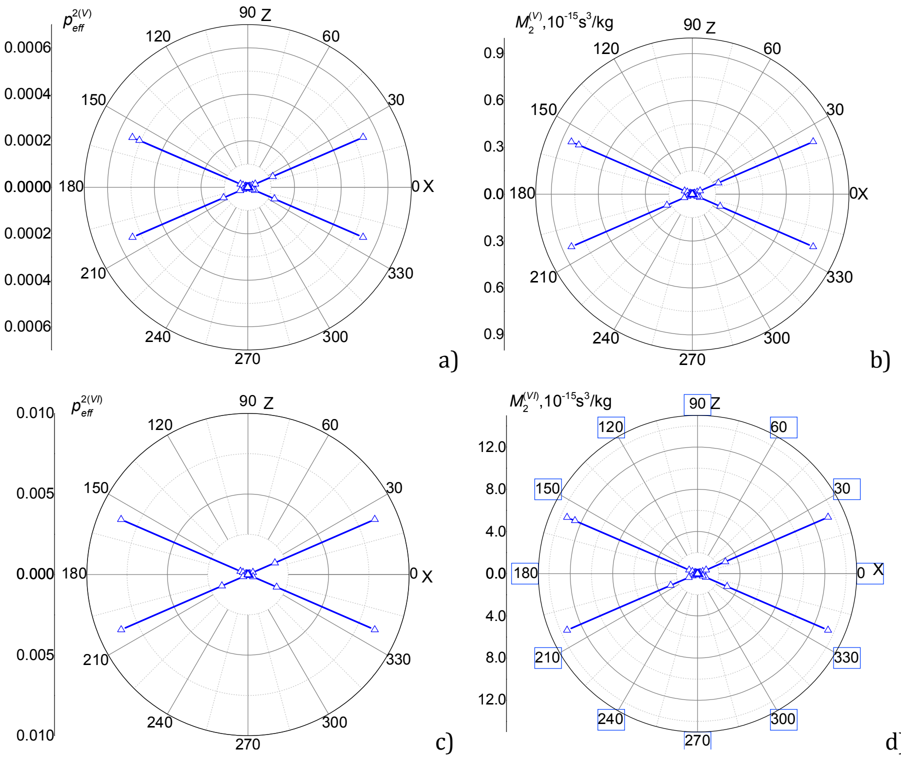

Fig. 4. Dependencies of effective EO coefficients (a, c) and AO figures of merit (b, d) on the angle θ_{ac} for the fifth (a, b) and sixth (c, d) types of AO interaction.

The dependencies of the effective EO coefficient and AO figures of merit for the fifth and sixth types of AO interactions are shown in Fig. 4. As seen in (Eqs. (18-21)), AO interactions with purely transverse waves polarized along the Y direction are forbidden without considering the ellipticity of the optical eigenwaves. Therefore, AO diffraction in these cases occurs only due to optical activity. Additionally, when a circularly polarized incident wave propagates along the optical axes, the AO figure of merit becomes quite high. Specifically, for the sixth type of AO interaction, the AO figure of merit reaches as high as 13.4×10^{-15} s^3/kg when the circularly polarized wave propagates along the optical axes (Fig. 4 c,d). Under the same conditions, the AO figure of merit is only 0.8×10^{-15} s^3/kg for the fifth type of AO interaction (Fig. 4a,b).

Table 1. Maximum values of the AO figure of merit with and without accounting for optical activity and polarization of the incident wave.

Type of AO interaction	**I**	**II**	**III**	**IV**	**V**	**VI**
AO figure of merit with accounting for optical activity, $10^{-15}s^3/kg$	23.7	23.8	45.6	46.4	0.8	13.4
AO figure of merit without accounting for optical activity, $10^{-15}s^3/kg$	10.8	11.9	45.6	46.4	-	-
Principal maximum value of the AO figure of merit for the interaction of linearly polarized optical waves, $10^{-15}s^3/kg$	28.1	34.3	46.3	74.0	-	-

The Table 1 presents the OA figure of merit for different types of AO interaction for comparison.

4. Conclusions

In this work, we have analyzed how the polarization of the incident optical wave affects the effective EO coefficient and the AO figure of merit in optically active, optically biaxial α-HIO_3 crystals. We find that both parameters increase when the polarization of the incident optical wave aligns with the polarization of the eigenwaves at the interaction with QL AW, when the incident optical wave propagates along one of the optical axes. At the first type of AO interaction, the AO figure of merit increases from 10.8×10^{-15} s^3/kg, the value typical for a linearly polarized wave, to 23.7×10^{-15} s^3/kg, characteristic of a circularly polarized wave, due to the incident wave's polarization as the eigenwave and propagates along the optical axis. The increase in AO figure of merit for these conditions leads to almost equality of this value with the maximal value of figure of merit observed in *XZ* interaction plane for incident linearly polarized optical wave, i.e., 28.1×10^{-15} s^3/kg, which occurs at θ_{ac}=90 and 270 deg. At the third and fourth types of AO interaction with QT_2 AW, the effect of optical activity on the AO figure of merit is negligibly small. However, the AO figure of merit for the fourth type of interaction reaches its maximum value within the *XZ* plane, i.e., 74.0×10^{-15} s^3/kg. The most intriguing phenomenon occurs at the fifth and sixth types of AO interactions with PT_2 AW. Under these conditions, AO diffraction is only possible due to the optical activity and ellipticity of the eigenwaves. In particular, for the sixth interaction type, the AO figure of merit caused solely by the eigenwaves' ellipticity reaches 13.4×10^{-15} s^3/kg.

Funding. This study was supported by the Ministry of Education and Science of Ukraine (project # 0125U002027).

Conflict of interest. Authors declare no conflict of interest.

References

1. Brillouin, L. (1922). Diffusion de la lumière et des rayons X par un corps transparent homogène. In *Annales de physique* (Vol. 9, No. 17, pp. 88-122).
2. Debye, P., & Sears, F. W. (1932). On the scattering of light by supersonic waves. *Proceedings of the National Academy of Sciences*, *18*(6), 409-414.
3. Lucas, R., & Biquard, P. (1932). Optical properties of solid and liquid medias subjected to high-frequency elastic vibrations. *Jour. De. Phys, et Rad*, *3*, 464-477.
4. Korpel, A. (1988). Acousto-Optics. Marcel Dekker. *Inc. New York and Basel*.
5. Balakshy, V. I., Parygin, V. N., & Chirkov, L. E. (1985). Physical principles of acousto-optics. *Radio i Svyaz, Moscow*.
6. Mys, O., Adamenko, D., Krupych, O., & Vlokh, R. (2018). Effect of deviation from purely transverse and longitudinal polarization states of acoustic waves on the anisotropy of acousto-optic figure of merit: the case of Tl_3AsS_4 crystals. *Applied Optics*, *57*(28), 8320-8330.
7. Buryy, O. A., Andrushchak, A. S., Kushnir, O. S., Ubizskii, S. B., Vynnyk, D. M., Yurkevych, Larchenko, O. V., Chaban, K. O., Gotra, O. Z., & Kityk, A. V. (2013). Method of extreme surfaces for optimizing geometry of acousto-optic interactions in crystalline materials: example of $LiNbO_3$ crystals. *Journal of Applied Physics*, *113*(8).

8. Mys, O., Kostyrko, M., Adamenko, D., Martynyuk-Lototska, I., Skab, I., & Vlokh, R. (2022). Effect of ellipticity of optical eigenwaves on the enhancement of efficiency of acousto-optic Bragg diffraction. A case of optically active $Pb_5Ge_3O_{11}$ crystals. *AIP Advances*, *12*(5).
9. Mys, O., Kostyrko, M., & Vlokh, R. (2024). Polarization of the Diffracted Optical Wave in the Crystals with Circular Optical Birefringence and Efficiency of Acousto-Optic Interaction Associated with Circularly Polarized Optical Waves in the Optically Active Crystals of Cubic System. *Ukrainian Journal of Physical Optics*, *25*(4), 04051-04062.
10. Krupych, O., Mys, O., Dudok, T., Say, A., & Vlokh, R. (2025). Effect of polarization ellipticity of the incident optical wave on acousto-optic diffraction efficiency and intensity modulation: case of TeO_2 crystals. *Applied Optics*, *64*(28), 8308-8313.
11. Sirotin, I. I., & Shaskol'skaia M. P. (1982). *Fundamentals of crystal physics*. MIR publishers.
12. Kurtz, S. K., Perry, T. T., & Bergman Jr, J. G. (1968). Alpha-iodic acid: A solution-grown crystal for nonlinear optical studies and application. *Applied Physics Letters*, *12*(5), 186-188.
13. Kupreychik, M. I., & Balakshy, V. I. (2017). The spatial structure of acousto-optic phase matching in biaxial crystal of alpha-iodic acid. *Optics and Spectroscopy*, *123*(3), 463-470.
14. Naito, H., & Inaba, H. (1972). Measurement of the refractive indices of α-iodic acid, HIO_3 crystal. *Opto-electronics*, *4*(3), 335-337.
15. Ivanov, N. R., & Chikhladze, O. A. (1976). Experimental determination of gyration in anorthorombic crystal α-HIO_3. *Kristallografiya*, *21*(1), 125-132.
16. Shaskolskaya, M.P. (1982). Acoustic crystals, *Nauka, Moscow*.
17. Nye, J. F. (1957). Physical Properties of Crystals (Oxford Univ. *Press (clarendon) London*.

Mys, O., Kostyrko, M., Vlokh, R. (2026). Polarization–Dependent Acousto-Optic Efficiency in Optically Active Biaxial α-HIO_3 Crystals. *Ukrainian Journal of Physical Optics*, *27*(1), 01110 – 01120. doi: 10.3116/16091833/Ukr.J.Phys.Opt.2026.01110

Анотація. *У цій роботі проаналізовано вплив поляризації вхідної оптичної хвилі на ефективний пружнооптичний коефіцієнт та коефіцієнт акустооптичної якості в оптично активних, оптично двовісних кристалах α-HIO_3. Виявлено, що при взаємодії з квазіпоздовжньою акустичною хвилею відбувається збільшення обох параметрів, у випадку коли поляризація вхідної оптичної хвилі збігається з поляризацією власних хвиль. При акустооптичній взаємодії з квазіпоздовжньою акустичною хвилею коефіцієнт акустооптичної якості зростає більш ніж удвічі, досягаючи майже такого ж значення, як максимальне значення цього коефіцієнта в площині акустооптичної взаємодії XZ. Було виявлено, що при п'ятому та шостому типах акустооптичної взаємодії з чистою поперечною акустичною хвилею акустооптична дифракція можлива лише завдяки оптичній активності та еліптичності власних хвиль. Зокрема, для шостого типу взаємодії коефіцієнт акустооптичної якості, зумовлений виключно еліптичністю власних хвиль, досягає $13,4\times10^{-15}$ с^3/кг.*

Ключові слова: *коефіцієнт акустооптичної якості, двовісні кристали, оптична активність, кристал α-HIO_3*